Journal of Physics B: Atomic, Molecular and Optical Physics

PAPER

Relativistic effects on the cross section and circular polarization of x-ray radiation following longitudinally-polarized electron impact excitation of highly charged ions

To cite this article: Z B Chen *et al* 2015 *J. Phys. B: At. Mol. Opt. Phys.* **48** 045202

IOP Publishing Journal of Physics B: Atomic, Molecular and Optical Physics
J. Phys. B: At. Mol. Opt. Phys. **48** (2015) 045202 (9pp) doi:10.1088/0953-4075/48/4/045202

Relativistic effects on the cross section and circular polarization of x-ray radiation following longitudinally-polarized electron impact excitation of highly charged ions

Z B Chen[1], J L Zeng[1] and C Z Dong[2]

[1] College of Science, National University of Defense Technology, Changsha, Hunan 410073, People's Republic of China
[2] Joint Laboratory of Atomic and Molecular Physics, Northwest Normal University and Institute of Modern Physics of Chinese Academy of Sciences and Northwest Normal University, Lanzhou 730070, People's Republic of China

E-mail: jlzeng@nudt.edu.cn

Received 28 August 2014
Accepted for publication 28 November 2014
Published 21 January 2015

Abstract

Detailed calculations using a fully relativistic distorted-wave method are carried out for the cross sections of longitudinally polarized electron impact excitation from the ground state to the magnetic sublevels of the $1s2p_{3/2}(J = 2)$ state of highly charged He-like ions. The relativistic effects on the cross sections and circular polarization of the x-ray photoemission are investigated in detail. For the excitation process, results show that the relativistic effects may become important leading to considerable enhancements in the cross sections. The inclusion of the relativistic effects can modify the cross sections by several orders of magnitude, especially to the $M_f = -1$ and -2 magnetic sublevels. For the de-excitation process, the relativistic effects make the degree of circular polarization decreases, these features are more pronounced when the incident electron energy and/or atomic number increase. The relativistic effects are found to be much larger compared to the case of the linear polarization of radiation.

Keywords: circular polarization, excitation cross sections, longitudinally-polarized-electron

1. Introduction

When highly charged ions are excited by a (directed) beam of electrons or, more generally, by electrons with a cylindrically symmetric but otherwise anisotropic velocity distribution, the excited state populations of the magnetic sublevels may exhibit nonstandard statistics [1]. Then, the radiation emitted from these unequally populated sublevels to a lower level is strongly polarized. The direction of this polarization is important not only for diagnosing the electron distribution anisotropy in high temperature plasmas, but also for providing information on the collision dynamics [2–8]. Based on these features, some diagnostic tools have been developed to characterize both the angular distribution and the polarization properties of x-ray emission [1, 4] in laboratory and astrophysical plasmas, particularly in solar corona, tokamak, and laser-produced plasmas.

Several studies have been carried out in the past to understand more clearly the angular and polarization properties of x-ray emission. With respect to experiments, Henderson *et al* [9] reported the first polarization measurements of x-rays emitted by bound–bound transitions in highly charged He-like Sc^{19+} ions. They concluded that the polarization is a useful feature for studying hyperfine interactions. Later, a series of other important polarization measurements were also reported [10–14]. With respect to theory, Chen *et al* [15] calculated the linear polarization of x-ray emission from the electron-impact excitation (EIE) of highly charged Ne-like Fe^{17+} ions using a Dirac *R*-matrix method. They discovered large differences, up to 30% or more, compared with earlier theoretical work. Reed *et al* [16] investigated the influence of relativistic effects on the linear polarization of x-rays emitted by the EIE of highly charged H-like and He-like ions. They

found that relativistic effects considerably alter the linear polarization. Wu *et al* [17] studied the degree of linear polarization of the two strongest 5f → 3d lines produced by EIE and the dielectronic recombination processes of Cu-like to Se-like gold ions. They pointed out that the significant differences between the polarizations from different formation processes can be employed to diagnose the formation mechanism of the corresponding lines. We [4] calculated the linear polarization and angular distribution of radiation following EIE of H-like and He-like ions. Results show that the $E1$–$M2$ interference effects can either decrease or enhance the line polarization for emitted x-rays, and these dramatic influences will also lead to a remarkable variation of the subsequent angular emission pattern. There are also many other theoretical studies on the polarization of x-ray emission [7, 18–34].

So far, however, most theoretical studies on the x-ray emission have dealt with a (spin)-unpolarized electron beam. As a consequence, the linear polarization of the radiation has been considered. As is well known, the excitation of ions by a polarized electron beam will lead in general to an orientation of the excited level; i.e., there will be an unequal population of the different M_J magnetic sublevels of the final level, particularly for those with opposite sign [23]. The radiation subsequently emitted in the decay of these oriented levels therefore exhibits not only linear polarization but also circular polarization [36]. For light- and medium-Z elements, early work on the impact excitation cross sections and circular polarization properties of the x-ray line emission was performed by Inal and co-workers [35–37]. In their investigations, the effects of the inner-shell ionization and the hyperfine interaction were studied for He-like ions using the fully relativistic distorted-wave (RDW) method. Results showed that the inner-shell ionization effects can increase the circular polarization above the ionization threshold. However, at higher impact energies, the inner-shell ionization has the effect of decreasing the degree of circular polarization [37]. Hereby, the main emphasis was only placed on relatively low-Z systems. To the best of our knowledge, there have been no previous theoretical calculations in the high-Z domain besides our own recent work [23]. In particular, since the polarization properties of the emitted radiation depend upon the cross sections for excitation to magnetic sublevels, one might also expect that relativistic effects would be significant for the cross sections and circular polarization of x-ray radiation created during impact excitation by longitudinally polarized electrons.

In this contribution, we apply the multi-configuration Dirac–Fock method and the fully RDW method [4, 7, 23, 34] to calculate cross sections for impact excitation by a longitudinally polarized electron beam. Special attention is paid to the contributions of the relativistic effects to the cross sections and circular polarization properties of subsequent x-ray radiation. To perform such an analysis, we computed two sets of cross sections for the $1s^2(J=0) \rightarrow 1s2p_{3/2}(J=2)$ excitation of highly charged He-like Fe^{24+}, Xe^{52+}, W^{72+}, and Pb^{80+} ions: the non-relativistic and the fully relativistic. Results for these cross sections and circular polarizations were compared in order to stress the relative importance of relativistic effects as the atomic number or incident energy increases. The plan of the paper is as follows. In section 2, we describe the theoretical approach and computational details. In section 3, we present our results for the cross sections and circular polarizations of x-ray radiation. Differences between the results of the non-relativistic and fully relativistic calculations are analyzed in terms of the atomic number and the incident energy [38]. Finally, we end with some conclusions in section 4.

2. Theory

In this study, the atomic structure data used in calculating fully RDW excitation cross sections were generated by the widely used atomic structure package GRASP92 [39] with the inclusion of a finite nuclear charge distribution and quantum electrodynamics (QED) corrections. For calculation of the excitation cross sections, in the present work, the quantization axis (z axis) is taken along the incident electron beam, so the z component of the incident electron orbital angular momentum $m_{l_i} = 0$. The subscript i refer to the initial states and the subscript f refer to the final states. The direct longitudinally polarized EIE cross section for scattering an electron accompanied by change in the state of the target atom/ion from $\beta_i J_i M_i$ to $\beta_f J_f M_f$ can be given by improving the formula [23, 35–37]

$$\begin{aligned}
&\sigma_{\varepsilon_i}\left(\beta_i J_i M_i - \beta_f J_f M_f\right) \\
&= \frac{2\pi a_0^2}{k_i^2} \cdot \sum_{l_i, l_i', j_i, j_i', m_{s_i}, l_f, j_f, m_f} \\
&\times \sum_{J, J', M} (i)^{l_i - l_i'} \left[\left(2l_i + 1\right)\left(2l_i' + 1\right)\right]^{1/2} \\
&\times \exp\left[i\left(\delta_{\kappa_i} - \delta_{\kappa_i'}\right)\right] C\left(l_i \frac{1}{2} m_{l_i} m_{s_i}; j_i m_i\right) \\
&\times C\left(l_i' \frac{1}{2} m_{l_i'} m_{s_i}; j_i' m_i\right) C\left(J_i j_i M_i m_i; JM\right) \\
&\times C\left(J_i j_i' M_i m_i; J'M\right) C\left(J_f j_f M_f m_f; JM\right) \\
&\times C\left(J_f j_f M_f m_f; J'M\right) R(\gamma_i, \gamma_f) R\left(\gamma_i', \gamma_f'\right),
\end{aligned} \tag{1}$$

where a_0 and ε_i is the Bohr radius and the incident energy, respectively. The C and R are Clebsch–Gordan coefficients and reactance matrix elements, respectively. δ_{κ_i} is the phase factor of the continuum electron.

$$\gamma_i = \varepsilon_i l_i j_i \beta_i J_i JM; \;\; \gamma_f = \varepsilon_f l_f j_f \beta_f J_f JM \tag{2}$$

in which J and M are the quantum numbers corresponding to the total angular momentum of the complete system, target ion plus free electron, and its z component, respectively. β_i and β_f represents other quantum numbers which required to specify the initial states and final states of the target ion in addition to its total angular momentum J_i and z component M_i, respectively. j_i and m_i are the total angular momentum and its z component of the incident electron, respectively; l_i is the orbital angular momentum of the incident electron. κ and k_i is

the relativistic quantum number and the relativistic wave number, respectively [7, 17]

$$k_i^2 = \varepsilon_i\left(1 + \frac{\alpha^2\varepsilon_i}{4}\right). \quad (3)$$

In which α is the fine-structure constant. The reactance matrix element $R(\gamma_i, \gamma_f)$ can be written as [7, 17]

$$R(\gamma_i, \gamma_f) = \left\langle \Psi_{\gamma_f} \middle| \sum_{p,q,p<q}^{N+1} \left(V_{\text{Coul}} + V_{\text{Breit}}\right) \middle| \Psi_{\gamma_i} \right\rangle, \quad (4)$$

where Ψ_{γ_i} are the initial states wavefunctions of the impact systems. Ψ_{γ_f} are the final states wavefunctions of the impact systems. V_{Breit} and V_{Coul} is the Breit interaction operator [39, 40] and the Coulomb interaction operator [7, 17], respectively.

The degree of circular polarization of the radiation is defined as [23, 35–37]

$$P_c = \frac{I_{\sigma^+} - I_{\sigma^-}}{I_{\sigma^+} + I_{\sigma^-}}, \quad (5)$$

where I_{σ^+} and I_{σ^-} are the intensities of the left- and right-handed circularly polarized radiation, respectively. If we assume that the target ions are devoid of hyperfine interactions and the incident electron beam is completely longitudinally polarized, then the polarization P_c observed in a direction along that of the electron beam can be expressed in terms of the populations. For radiation from the $J = 2$ level to the $J = 0$ level, the circular polarization is given by [23, 35–37]

$$P_c = \frac{\sigma_1 - \sigma_{-1}}{\sigma_1 + \sigma_{-1}}, \quad (6)$$

where σ_1 and σ_{-1} are the excitation cross sections from the ground state to the magnetic sublevels $M_f = 1$ and -1 of the excited state, respectively.

3. Results and discussions

In order to obtain accurate atomic energy levels and wave functions of the initial and final states, the contributions of the Breit interaction and QED corrections are taken into account [7, 17]. In the calculation of cross sections, the maximal partial-wave $\kappa = 90$ is included to ensure convergence. In table 1, the calculated collision strengths for longitudinally polarized electron excitation from the ground level to the different magnetic sublevels of the 1s2p and 1s3p levels of He-like Fe^{24+} ions are shown and compared with the available theoretical values [23, 35]. It can be seen that the present relativistic results are in very good agreement with the existing theoretical results. Taking the $1s^2(J = 0) \rightarrow 1s2p_{3/2}$ $(J = 1)$ excitation, for example, the present collision strengths are 1.42×10^{-3}, 3.74×10^{-3}, and 1.33×10^{-3} for the $M_f = -1$, 0, and 1 magnetic sublevels, respectively. Compared with the fully relativistic theoretical results 1.33×10^{-3}, 3.82×10^{-3}, and 1.25×10^{-3}, and the semi-relativistic results 1.38×10^{-3}, 3.79×10^{-3}, and 1.30×10^{-3} given by Inal *et al* [35], respectively, we have a discrepancy of less than 8%. But a rather large discrepancy occur between semi-relativistic and fully relativistic calculations for the transitions to the magnetic sublevel $M_f = -2$. The reason can be seen clearly from [35]. Moreover, the present circular polarizations are also in very good agreement with the results calculated by Inal *et al* [35], as listed in table 2.

To show further the reliability of our present calculations in the high-Z domain, in table 3 we list the calculated collision strengths for unpolarized EIE from the ground state to the magnetic sublevels of the 1s2p levels of He-like Xe^{52+} ions, and compare them with the theoretical predictions of Fontes *et al* [28], who used the fully relativistic method with (first column) and without (second column) the generalized Breit interaction. Inspection of table 3 shows that the values obtained by the two approaches do not differ substantially. The present collision strengths also agree very well with these relativistic results.

Figure 1 shows the total cross sections from the ground state to the excited state $1s2p_{3/2}(J = 2)$ for He-like Fe^{24+}, Xe^{52+}, W^{72+}, and Pb^{80+} ions as a function of incident electron energy in threshold units. To emphasize the contributions of the relativistic effects, here, we computed two sets of cross sections with (labeled by R) and without (labeled by NR) relativistic effects included, respectively. In our non-relativistic calculation, we select the speed of light to be 10 000 a.u. instead of the default value 137.036 a.u. in the GRASP92 program [7] and the RDW program. As shown in figure 1, both total cross sections with and without the relativistic effects decrease monotonically in a similar fashion as the incident energy increases: they decrease rapidly at the threshold energy then more slowly at higher energies [7]. As expected, for the low-Z Fe^{24+} ions, differences between the total cross sections with and without relativistic effects are small, they do not exceed 20% even at five times the threshold energy [38]. The relativistic effects tend to make the total cross sections increase over the whole energy range considered, becoming more pronounced with increase of the incident electron energy and/or atomic number. Their contribution to the total cross sections is about 5, 24, 64, and 85% at 1.5 times the threshold energy and 16, 120, 380, and 580% at five times the threshold energy for highly charged He-like Fe^{24+}, Xe^{52+}, W^{72+}, and Pb^{80+} ions, respectively.

The $M_f = 0$ sublevel cross sections are provided in figure 2. It is can be seen the $M_f = 0$ sublevel cross sections follow a trend very similar to that of the total cross sections. The relativistic effects also make the cross sections increase [7, 23], becoming more pronounced with increase of the incident electron energy and/or atomic number.

Figure 3 shows the $M_f = \pm 2$ sublevel cross sections for He-like Fe^{24+}, Xe^{52+}, W^{72+}, and Pb^{80+} ions as a function of incident longitudinally polarized electron energy. In the case where relativistic effects are not taken into account, it can be seen that both the $M_f = 2$ and -2 cross sections decrease slowly with increasing incident energy. The $M_f = 2$ sublevel remains preferentially populated relative to $M_f = -2$ in all the

Table 1. Comparison of collision strengths for excitation from the ground level to the different magnetic sublevels of the 1s2p and 1s3p levels of He-like Fe^{24+} ions by longitudinally polarized electrons. The incident energy is 1200 Ry. The two sets of results for the $1s2p_{3/2}(J = 2)$ level pertain to the two kinds of theoretical calculation in [37]. Here $R[n]$ means $R \times 10^n$.

Excited state	M_f	Relativistic	Semi-relativistic	Present
$1s2p_{1/2}(J = 0)$	0	5.17[−5][a], 5.27[−5][c]		4.76[−5]
$1s2p_{3/2}(J = 2)$	−2	3.63[−9][a], 1.82[−7][a], 3.60[−9][b], 4.02[−9][c]	2.56[−18][b]	1.86[−7]
	−1	1.08[−5][a], 1.52[−5][a], 1.08[−5][b], 1.14[−5][c]	1.07[−5][b]	1.59[−5]
	0	7.35[−5][a], 8.19[−5][a], 7.33[−5][b], 7.55[−5][c]	7.51[−5][b]	8.36[−5]
	1	1.10[−4][a], 1.10[−4][a], 1.10[−4][b], 1.16[−4][c]	1.13[−4][b]	1.15[−4]
	2	4.23[−5][a], 4.44[−5][a], 4.21[−5][b], 4.49[−5][c]	4.28[−5][b]	4.74[−5]
$1s2p_{1/2}(J = 1)$	−1	8.20[−5][b], 8.27[−5][c]	6.56[−5][b]	8.98[−5]
	0	3.78[−4][b], 3.80[−4][c]	3.37[−4][b]	3.54[−4]
	1	2.83[−4][b], 2.87[−4][c]	2.62[−4][b]	3.22[−4]
$1s2p_{3/2}(J = 1)$	−1	1.33[−3][b], 1.39[−3][c]	1.38[−3][b]	1.42[−3]
	0	3.82[−3][b], 3.94[−3][c]	3.79[−3][b]	3.74[−3]
	1	1.25[−3][b], 1.30[−3][c]	1.30[−3][b]	1.33[−3]
$1s3p_{1/2}(J = 0)$	0			1.76[−5]
$1s3p_{3/2}(J = 2)$	−2	1.22[−9][b]	4.84[−13][b]	3.56[−7]
	−1	3.23[−6][b]	3.25[−6][b]	3.67[−6]
	0	2.41[−5][b]	2.52[−5][b]	3.32[−5]
	1	3.60[−5][b]	3.78[−5][b]	3.64[−5]
	2	1.25[−5][b]	1.30[−5][b]	1.43[−5]
$1s3p_{1/2}(J = 1)$	−1	1.23[−5][b]	1.08[−5][b]	1.89[−5]
	0	7.22[−5][b]	6.49[−5][b]	7.01[−5]
	1	6.80[−5][b]	6.41[−5][b]	7.12[−5]
$1s3p_{3/2}(J = 1)$	−1	2.13[−4][b]	2.17[−4][b]	2.20[−4]
	0	6.54[−4][b]	6.44[−4][b]	6.46[−4]
	1	1.96[−4][b]	1.98[−4][b]	2.02[−4]

[a] Reference [37].
[b] Reference [35].
[c] Reference [23].

Table 2. Degree of circular polarization for the lines $1snp(J = 1, 2) \rightarrow 1s^2(J = 0)$ $(n = 2, 3)$ of He-like Fe^{24+} ions. For the three lines with $n = 2$, we compare our present results (upper entries) with the fully relativistic (second entries) and semirelativistic (third entries) results obtained by Inal *et al* [35].

	Energy(Ry)				
Transition	550	900	1200	2000	5000
$1s2p_{3/2}(J = 1) \rightarrow 1s^2(J = 0)$	−0.086	−0.044	−0.033	−0.014	−0.004
	−0.088	−0.046	−0.031	−0.015	−0.004
	−0.097	−0.048	−0.030	−0.013	−0.004
$1s2p_{3/2}(J = 2) \rightarrow 1s^2(J = 0)$	0.836	0.833	0.820	0.765	0.580
	0.838	0.835	0.822	0.767	0.583
	0.843	0.842	0.826	0.770	0.590
$1s2p_{1/2}(J = 1) \rightarrow 1s^2(J = 0)$	0.955	0.762	0.556	0.251	0.065
	0.953	0.760	0.551	0.249	0.063
	0.957	0.778	0.600	0.273	0.069
$1s3p_{3/2}(J = 1) \rightarrow 1s^2(J = 0)$		−0.064	−0.043	−0.022	−0.001
$1s3p_{3/2}(J = 2) \rightarrow 1s^2(J = 0)$		0.848	0.817	0.783	0.602
$1s3p_{1/2}(J = 1) \rightarrow 1s^2(J = 0)$		0.873	0.580	0.335	0.082

He-like ions and over the whole energy range considered. When the relativistic effects are taken into account, it is found that they cause the $M_f = \pm 2$ sublevel cross sections to increase, and their influence becomes stronger for higher incident electron energies and/or atomic numbers, especially to the $M_f = -2$ sublevel. Taking the He-like W^{72+} ions as an example, the $M_f = -2$ sublevel cross sections are enhanced by as much as a factor of 36000, while the change is only a factor of 5 for excitation to the $M_f = 2$ sublevel at four times the threshold energy.

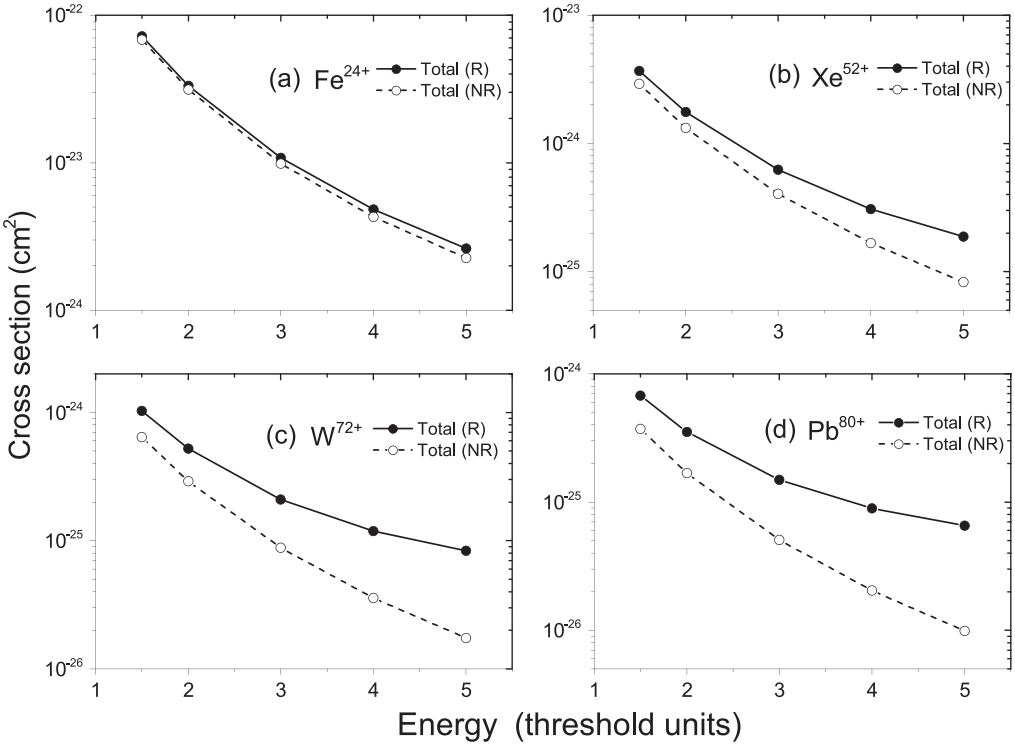

Figure 1. Total cross section for EIE from the ground state $1s^2(J = 0)$ to the excited state $1s2p_{3/2}(J = 2)$ for He-like Fe^{24+}, Xe^{52+}, W^{72+}, and Pb^{80+} ions as a function of incident energy in threshold units. NR and *R* represent the values without and with inclusion of relativistic effects, respectively.

Table 3. Comparison of collision strengths for excitation from the ground level to the different magnetic sublevels of the 1s2p levels of He-like Xe^{52+} ions by unpolarized electron. The incident electron energy is 4000 Ry. The two sets of results pertain to the two kinds of theoretical calculations in [28]. Here $R[n]$ means $R \times 10^n$.

Excited state	M_f	Reference [28]	Present
$1s2p_{1/2}(J = 0)$	0		1.803[−5]
$1s2p_{3/2}(J = 2)$	2	9.879[−6], 8.078[−6]	9.829[−6]
	1	2.743[−5], 2.364[−5]	2.722[−5]
	0	4.031[−5], 2.874[−5]	4.007[−5]
	Total	1.149[−4], 9.219[−5]	1.142[−4]
$1s2p_{1/2}(J = 1)$	1	1.153[−4], 9.230[−5]	1.145[−4]
	0	2.007[−4], 2.426[−4]	2.004[−4]
	Total	4.314[−4], 4.272[−4]	4.294[−4]
$1s2p_{3/2}(J = 1)$	1	1.706[−4], 1.589[−4]	1.699[−4]
	0	4.829[−4], 5.540[−4]	4.762[−4]
	Total	8.241[−4], 8.717[−4]	8.160[−4]

In figure 4, we show the $M_f = \pm 1$ sublevel cross sections for excitation to the excited state $1s2p_{3/2}(J = 2)$ for He-like Fe^{24+}, Xe^{52+}, W^{72+}, and Pb^{80+} ions as a function of incident longitudinally polarized electron energy. For heavy ions, a general phenomenon is that the relativistic effects make a relatively large contribution to the $M_f = -1$ cross sections for direct excitation of heavy atomic ions by longitudinally polarized electron impact. For example, without the contributions of relativistic effects, both the $M_f = 1$ and -1 cross sections decrease slowly with increasing incident electron energy. The cross sections for excitation to magnetic sublevel $M_f = 1$ are much larger than those to the sublevel $M_f = -1$ at a given incident energy [7, 23]. When relativistic effects are taken into account, it is also found that the $M_f = \pm 1$ sublevel cross sections increase. The effect for excitation to $M_f = -1$ is large, while that for $M_f = 1$ is small. Taking He-like W^{72+} ions as an example, the $M_f = -1$ sublevel cross sections are increased by as much as a factor of 15, but only by a factor of 1.3 for excitation to the $M_f = 1$ sublevel at four times the threshold energy. Moreover, it is worth mentioning that the $M_f = \pm 1$ sublevels cross section curves cross each other at about 3.2 and 2.7 times the threshold energy for He-like W^{72+} and Pb^{80+} ions, respectively [7].

In figure 5, we show the circular polarization of the $1s2p_{3/2}(J = 2) \rightarrow 1s^2(J = 0)$ line for He-like Fe^{24+}, Xe^{52+}, W^{72+}, and Pb^{80+} ions as a function of the incident longitudinally polarized electron energy. It is can be seen that the circular polarization is large and decreases very slowly as the incident energy increases, while the circular polarization rapidly decreases for all ions at any given incident energy when relativistic effects are taken into account.

It appears that the relativistic effects in our calculations might be due to the relativistic effects on the atomic structure of the target ions [16]. To test this, we repeated the calculations of the circular polarization for He-like W^{72+} ions taking relativistic effects into account for the target structure calculation but not for the scattering calculation. The results are presented in figure 5(c). It can be seen that the curve is closer to the non-relativistic curve at all given incident energies, thus

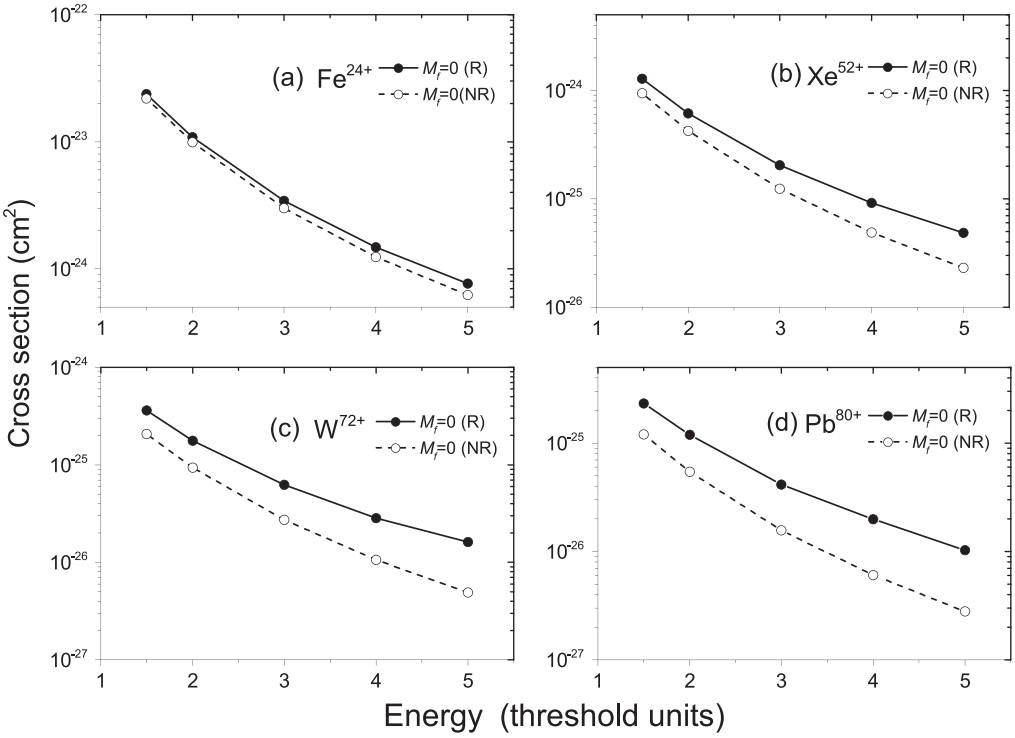

Figure 2. $M_f = 0$ magnetic sublevel cross section for longitudinally polarized EIE from the ground state $1s^2(J = 0)$ to the excited state $1s2p_{3/2}$ $(J = 2)$ for He-like Fe^{24+}, Xe^{52+}, W^{72+}, and Pb^{80+} ions as a function of incident energy in threshold units. NR and *R* represent the values without and with inclusion of relativistic effects, respectively.

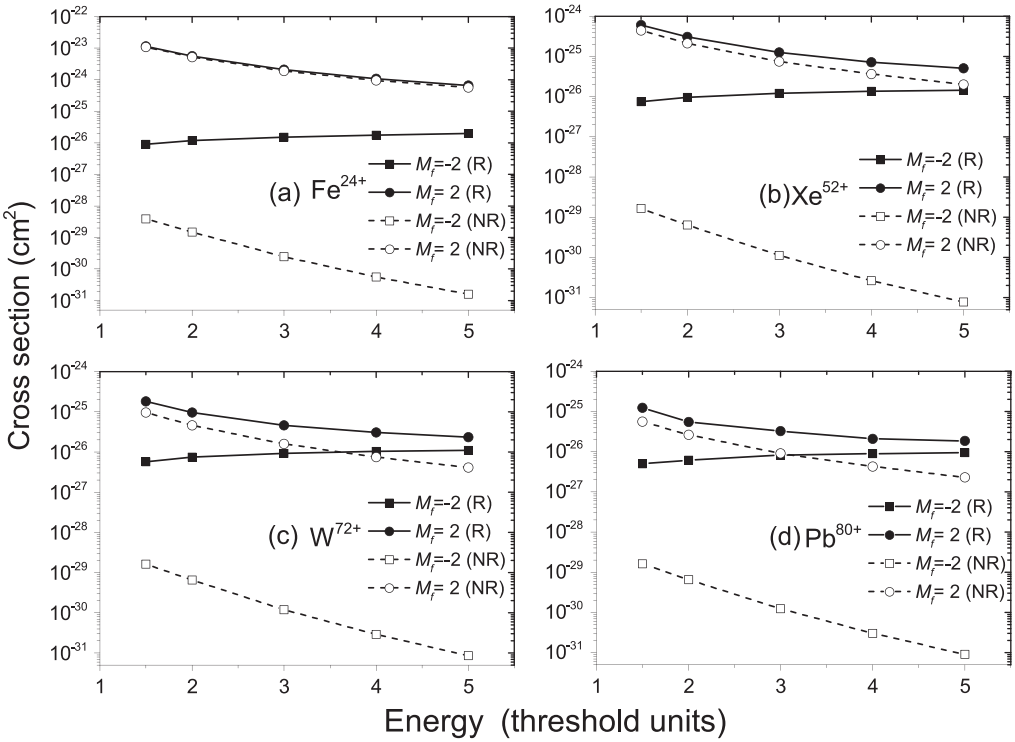

Figure 3. The same as in figure 2, but for $M_f = \pm 2$ magnetic sublevels.

demonstrating that relativistic effects on the target structure are not significant. Furthermore, to assess the contributions of the Breit interaction, we calculated the circular polarization of He-like Xe^{52+} ions using the relativistic method but not including the Breit interaction. The results are shown in figure 5(b), where we can see that the Breit interaction has a considerable influence on the polarization, and that the resulting changes become progressively more significant as

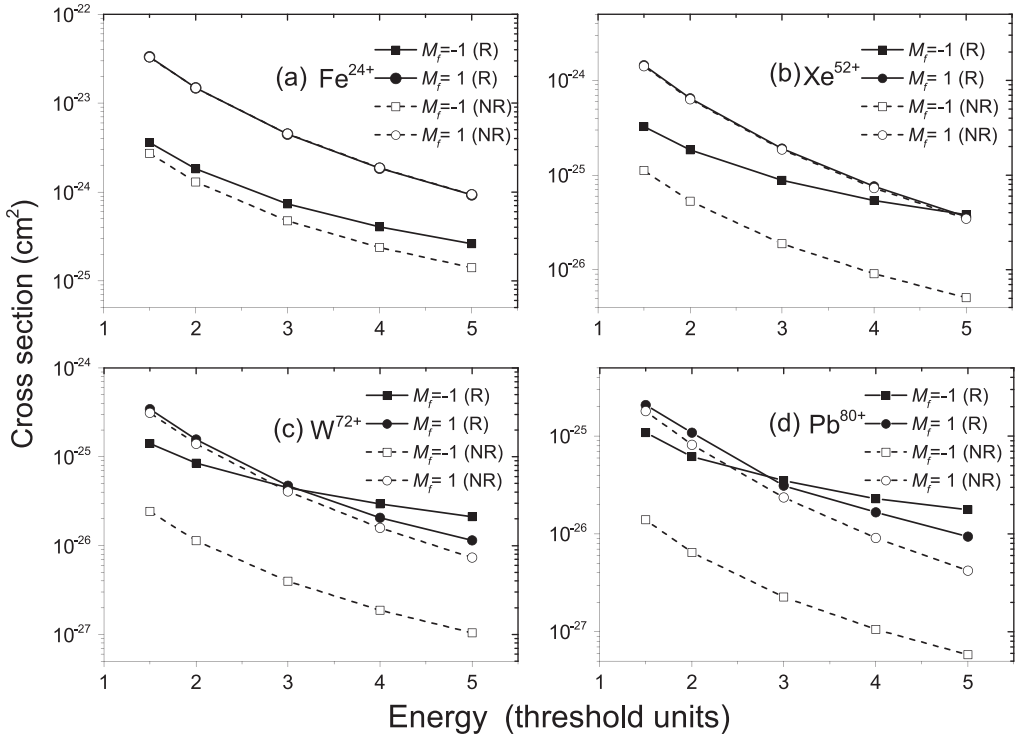

Figure 4. The same as in figure 2, but for $M_f = \pm 1$ magnetic sublevels.

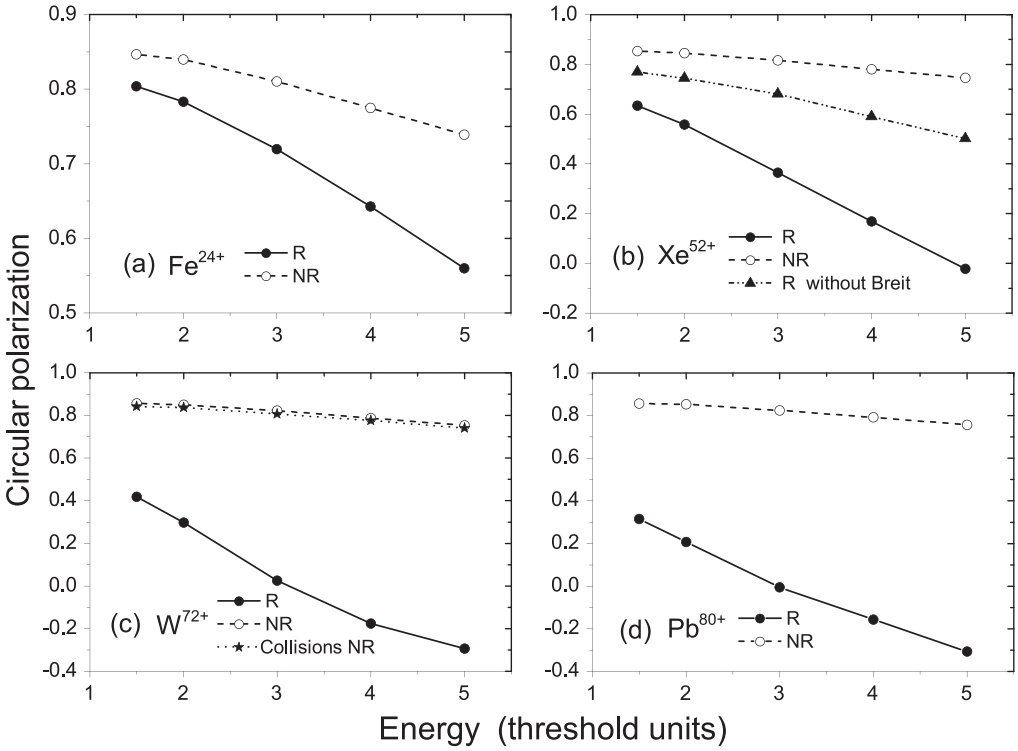

Figure 5. The degree of circular polarization of the transition line $1s2p_{3/2}(J = 2) \rightarrow 1s^2(J = 0)$ for He-like Fe^{24+}, Xe^{52+}, W^{72+}, and Pb^{80+} ions as functions of incident energy in threshold units. NR represents the values without inclusion of relativistic effects, and *R* represents the ones with the relativistic effects included.

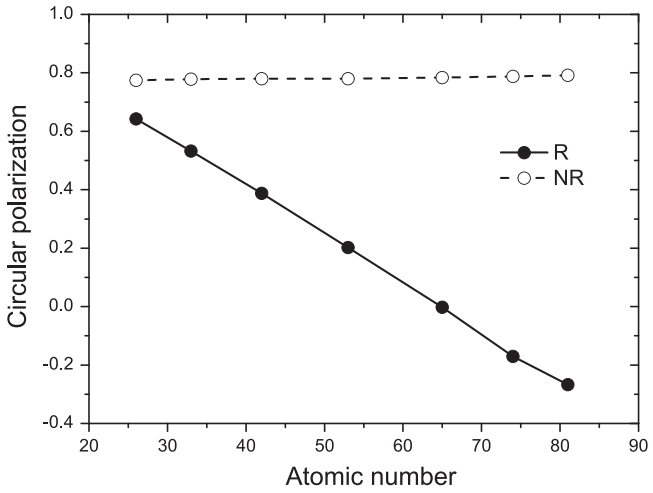

Figure 6. Degree of circular polarization of the transition line $1s2p_{3/2}$ $(J = 2) \rightarrow 1s^2 (J = 0)$ for He-like ions as a function of atomic number at an incident energy of four times the threshold energy. NR and *R* represent the values without and with inclusion of relativistic effects, respectively.

the incident energy increases. Therefore, for scattering calculations, the Breit interaction is a dominant factor in the process of longitudinally polarized EIE of highly charged ions.

Finally, in figure 6, we display the degree of circular polarization with and without the relativistic effects included as a function of the atomic number at a given incident energy (four times the threshold energy). It is evident that, due to the relativistic effect, the circular polarization decreases for all the He-like ions with the atomic number increasing. However, with/without relativistic effects included, it decreases rapidly/very slowly. All these features are found to be much more pronounced compared to the case of the linear polarization of radiation emitted by an unpolarized EIE process [16].

In the above sections, we have studied the relativistic effects on the cross sections and the circular polarizations of x-ray radiation emitted by direct impact excitation. Besides the direct impact excitation, some other effects such as the radiative cascades from higher excited levels and the resonance impact excitation may greatly affect the excitation cross sections and the circular polarizations of the corresponding line in some cases [35]. These effects are neglected in the present work and some detailed calculations will be done in future works.

4. Conclusions

In summary, longitudinally polarized EIE cross sections and the circular polarization of x-ray radiation of the $1s2p_{3/2}$ $(J = 2) \rightarrow 1s^2 (J = 0)$ line of He-like Fe^{24+}, Xe^{52+}, W^{72+}, and Pb^{80+} ions are calculated using the fully RDW method, including a detailed analysis of the influence of relativistic effects. It is found that, due to the relativistic effects, both total and magnetic sublevel cross sections increase, with a very large increase for excitation to the $M_f = -1, -2$ sublevel cross sections but a relatively small increase for the total and $M_f = 0, 1, 2$ sublevels. For example, for He-like W^{72+} ions, the relativistic effects increase the $M_f = -1$ sublevel cross sections by as much as a factor of 15, but only by a factor of 1.3 for the $M_f = 1$ sublevel at four times the threshold energy. Again, the $M_f = -2$ sublevel cross sections increase by as much as a factor of 36 000, but only by a factor of 5 for the $M_f = 2$ sublevel at four times the threshold energy. It is also found that, due to relativistic effects, the degree of circular polarization decreases at a given incident electron energy. These features are more pronounced for higher incident electron energies and/or atomic numbers. All these effects are found to be much larger for circular polarization than for linear polarization of radiation emitted during an unpolarized EIE process.

Acknowledgments

The authors acknowledge the support of the National Natural Science Foundation of China (Grant Nos. 11274382, U1332206, and 11274254).

References

[1] Shi Y L, Dong C Z, Ma X Y, Wu Z W, Xie L Y and Fritzsche S 2013 *Chin. Phys. Lett.* **30** 063401
[2] Beiersdorfer P *et al* 1996 *Phys. Rev.* A **53** 3974
[3] Inal M K and Dubau J 1993 *Phys. Rev.* A **47** 4794
[4] Chen Z B, Dong C Z, Xie L Y and Jiang J 2014 *Phys. Rev.* A **90** 012703
[5] Shlyaptseva A S, Mancini R C, Neill P and Beiersdorfer P 1997 *Rev. Sci. Instrum.* **68** 1095
[6] Inal M K and Dubau J 1987 *J. Phys. B: At Mol. Phys.* **20** 4221
[7] Wu Z W, Jiang J and Dong C Z 2011 *Phys. Rev.* A **84** 032713
[8] Takács E *et al* 1996 *Phys. Rev.* A **54** 1342
[9] Henderson J R *et al* 1990 *Phys. Rev. Lett.* **65** 705
[10] Nakamura N, Kato D, Miura N, Nakahara T and Ohtani S 2001 *Phys. Rev.* A **63** 024501
[11] Walden F, Kunze H-J, Petoyan A, Urnov A and Dubau J 1999 *Phys. Rev.* E **59** 3562
[12] Robbins D L *et al* 2006 *Phys. Rev.* A **74** 022713
[13] Beiersdorfer P, Brown G, Utter S, Neill P, Reed K J, Smith A J and Thoe R S 1999 *Phys. Rev.* A **60** 4156
[14] Liu Y M, Singha S, Witt T E, Cheng Y T and Gordon R J 2008 *Appl. Phys. Lett.* **93** 161502
[15] Chen G X, Kirby K, Brickhouse N S, Lin T and Silver E 2009 *Phys. Rev.* A **79** 062715
[16] Reed K J and Chen M H 1993 *Phys. Rev.* A **48** 3644
[17] Wu Z W, Dong C Z and Jiang J 2012 *Phys. Rev.* A **86** 022712
[18] Sharma L, Surzhykov A, Srivastava R and Fritzsche S 2011 *Phys. Rev.* A **83** 062701
[19] Bostock C J, Fursa D V and Bray I 2009 *Phys. Rev.* A **80** 052708
[20] Amaro P, Fratini F, Fritzsche S, Indelicato P, Santos J P and Surzhykov A 2012 *Phys. Rev.* A **86** 042509
[21] Nakamura N, Kavanagh A P, Watanabe H, Sakaue H A, Li Y, Kato D, Currell F J and Ohtani S 2008 *Phys. Rev. Lett.* **100** 073203
[22] Hu Z, Han X, Li Y, Kato D, Tong X and Nakamura N 2012 *Phys. Rev. Lett.* **108** 073002

[23] Chen Z B, Dong C Z and Jiang J 2014 *Phys. Rev.* A **90** 022715
[24] Gumberidze A *et al* 2013 *Phys. Rev. Lett.* **110** 213201
[25] Fritzsche S, Surzhykov A and Stölker T 2009 *Phys. Rev. Lett.* **103** 113001
[26] Jiang J, Dong C Z, Xie L Y and Wang J G 2008 *Phys. Rev.* A **78** 022709
[27] Bernhardt D *et al* 2011 *Phys. Rev.* A **83** 020701(R)
[28] Fontes C J, Zhang H L and Sampson D H 1999 *Phys. Rev.* A **59** 295
[29] Kai T, Srivastava R and Nakazaki S 2004 *Phys. Rev.* A **70** 062705
[30] Inal M K, Surzhykov A and Fritzsche S 2005 *Phys. Rev.* A **72** 042720
[31] Kai T, Nakazaki S, Kawamura T, Nishimura H and Mima K 2007 *Phys. Rev.* A **75** 012703
[32] Chen M H and Scofield J H 1995 *Phys. Rev.* A **52** 2057
[33] Kai T, Nakazaki S, Kawamura T, Nishimura H and Mima K 2007 *Phys. Rev.* A **75** 062710
[34] Jiang J, Dong C Z, Xie L Y, Wang J G, Yan J and Fritzsche S 2007 *Chin. Phys. Lett.* **24** 691
[35] Inal M K, Zhang H L and Sampson D H 1992 *Phys. Rev.* A **46** 2449
[36] Inal M K, Sampson D H, Zhang H L and Dubau J 1997 *Phys. Scr.* **55** 170
[37] Inal M K, Zhang H L, Sampson D H and Fontes C J 2002 *Phys. Rev.* A **65** 032727
[38] Bettadj L, Inal M K and Benmouna M 2014 *J. Phys. B: At. Mol. Phys.* **47** 105205
[39] Parpia F A, Fischer C F and Grant I P 1996 *Comput. Phys. Commun.* **94** 249
[40] Fritzsche S, Aksela H, Dong C Z, Heinäsmäki S and Sienkiewicz J E 2003 *Nucl. Instrum. Methods Phys. Res.* B **205** 93